Superior Bone Microarchitecture in Anatomic Versus Nonanatomic Fibular Drill Tunnels for Reconstruction of the Posterolateral Corner of the Knee

Julian Stürznickel,*† MD, Felix N. Schmidt,† MD, PhD, Conradin Schweizer,* MD, Herbert Mushumba,‡ MD, Matthias Krause,*§ MD, Klaus Püschel,‡ MD, and Tim Rolvien,*§ MD, PhD

Investigation performed at the University Medical Center Hamburg-Eppendorf, Hamburg, Germany

Background: Several fibula-based reconstruction techniques have been introduced to address ligamentous injuries of the posterolateral corner of the knee. These techniques involve a drill tunnel with auto- or allograft placement through the proximal fibula.

Purpose: To determine the skeletal microarchitecture of the proximal fibula and its association with age and to compare the microarchitecture within the regions of different drill tunnel techniques for reconstruction of the posterolateral corner.

Study Design: Descriptive laboratory study.

Methods: A total of 30 human fibulae were analyzed in this cadaveric imaging study. High-resolution peripheral quantitative computed tomography measurements were performed in a 4.5 cm–long volume of interest at the proximal fibula. Three-dimensional microarchitectural data sets of cortical and trabecular compartments were evaluated using customized scripts. The quadrants representing the entry and exit drill tunnel positions corresponding to anatomic techniques (LaPrade/Arciero) and the Larson technique were analyzed. Linear regression models and group comparisons were applied.

Results: Trabecular microarchitecture parameters declined significantly with age in women but not men. Analysis of subregions with respect to height revealed stable cortical and decreasing trabecular values from proximal to distal in both sexes. Along with a structural variability in axial slices, superior values were found for the densitometric and microarchitectural parameters corresponding to the fibular drill tunnels in the anatomic versus Larson technique (mean ± SD; bone volume to tissue volume at the entry position, 0.273 ± 0.079 vs 0.175 ± 0.063; $P < .0001$; cortical thickness at the entry position, 0.501 ± 0.138 vs 0.353 ± 0.081 mm; $P < .0001$).

Conclusion: Age represented a relevant risk factor for impaired skeletal microarchitecture in the proximal fibula in women but not men. The region of drill tunnels according to anatomic techniques showed superior bone microarchitecture versus that according to the Larson technique.

Keywords: bone microarchitecture; HR-pQCT; knee; posterolateral corner; proximal fibula

The posterolateral corner (PLC) of the knee contributes to stabilization against varus forces as well as external tibial rotation and posterior tibial translation.[31] Injuries of the PLC are often undiagnosed, although they have been reported to occur in around 16% of all knee injuries.[18] The PLC is often involved in cruciate ligament injuries.[31] Clinically, a PLC injury may result in posterolateral rotational instability, chronic pain, failure of cruciate ligament reconstruction, and osteoarthritis.[31]

The proximal fibula (ie, fibular head) represents the attachment point of the lateral collateral ligament and the popliteofibular ligament. While a variety of PLC reconstruction options have been proposed, several fibula-based surgical techniques have been introduced to address PLC injuries.[10] These techniques involve a drill tunnel with auto- or allograft placement through the proximal fibula. Two of the most performed techniques for PLC reconstruction are the Arciero (fibula based) and LaPrade (tibia

The Orthopaedic Journal of Sports Medicine, 10(9), 23259671221126475
DOI: 10.1177/23259671221126475

and fibula based), representing nearly anatomic reconstruction techniques with an ascending fibular drill tunnel in the anterolateral-to-posteromedial direction.[1,11,28] Another commonly performed fibula-based reconstruction technique is the isometric Larson technique, in which a nonascending drill tunnel is positioned more distally and in the anterior-to-posterior direction.[19]

Although PLC reconstruction techniques are well established and have been shown to adequately restore varus and external rotation stability to the knee,[9] bone-related failure may occur (eg, intraoperative fracture, tunnel widening, cutout of the graft).[21,24] However, microarchitectural data on the proximal fibula overall are not available, let alone derived recommendations of fibula-based tunnel orientation. High-resolution peripheral quantitative computed tomography (HR-pQCT) represents an established technique to evaluate the microarchitectural features of different skeletal regions at a high spatial resolution (31 μm voxel size), which has been used in clinical practice and experimental cadaveric studies.[16,29]

The aim of the present study was to characterize the overall bone microarchitecture of the proximal fibula by HR-pQCT with respect to age and sex and to provide the underlying microarchitectural basis for drill tunnel orientation of nearly anatomic (ie, anatomic) and nonanatomic fibula-based PLC reconstruction techniques. The hypothesis was that age is a relevant risk factor for poor microarchitecture and that trabecular and cortical parameters vary within subregions of the proximal fibula, which may have implications for optimal drill tunnel positions.

METHODS

In total, 30 whole fibulae of the right leg were collected from 30 individuals during autopsy, consisting of 15 women and 15 men (mean ± SD; age, 51.7 ± 20.0 years [range, 18-87 years] and 51.5 ± 18.5 years [range, 24-76 years], respectively; $P = .985$). Hospital and autopsy reports were reviewed to exclude individuals with diseases potentially affecting skeletal integrity (eg, cancer, diabetes, glucocorticoid medication, or periods of longer immobilization) as well as previous surgical procedures around the knee joint.[25] Demographic data were recorded, including sex, age, and body mass index (BMI). All specimens were fixed in 3.7% formaldehyde within 48 hours after death. Informed consent was obtained from the relatives. This cadaveric study was approved by the local ethics committee and complied with the Declaration of Helsinki guidelines.

High-Resolution Peripheral Quantitative Computed Tomography

HR-pQCT measurements (XtremeCT II; Scanco Medical AG) were performed at a volume of interest (VOI) along the most proximal 4.5 cm of the proximal fibular tip with respect to the long axis of the bone using an ex vivo protocol (60 kVp, 900 μA, 100-ms integration time, 42-μm voxel size).[14] For optimal standardization, all scans were acquired by the same trained researcher (J.S.). All specimens were positioned with the same orientation and fixed within the manufacturer's cast to prevent motion artifacts. A standard evaluation protocol provided by the manufacturer was used to generate 3-dimensional microarchitectural data sets of the cortical and trabecular compartment. Consistent quality of the scans was controlled daily by using the manufacturer's calibration phantom.

We assessed the following parameters according to current guidelines[32]:

Densitometric—volumetric total bone mineral density (Tt.BMD), trabecular BMD (Tb.BMD), and cortical BMD (Ct.BMD)

Bone microarchitectural—bone volume to tissue volume (BV/TV), trabecular number (Tb.N), trabecular thickness, cortical thickness (Ct.Th), and cortical porosity

Geometric—total area, trabecular area, cortical area, and cortical perimeter.

VOI Analysis and Simulation of Tunnel Positions

Next to the measurement of bone microarchitecture parameters in the whole proximal fibula, 4 VOI subregions within the metaepiphysis representing different heights (ie, proximal to distal) were generated. The most proximal slice with a visible trabecular structure and the slice at the most distal point of the former growth line were identified. The number of slices between these points was measured and divided by 3 to get the number of slices for VOIs 1 to 3 proximal of the former growth line. For VOI 4, the same number of slices was added distal to the identified growth line.

Within each VOI, the corresponding slices from the proximal 25% to the distal 75% were selected for final analysis. Densitometric and microarchitectural parameters in the VOI subregions were analyzed using customized Python-based scripts. Moreover, specific quadrants representing the entry and exit points of drill tunnels according to the anatomic techniques and nonanatomic fibula-based

§Address correspondence to Tim Rolvien, MD, PhD, and Matthias Krause, MD, Department of Trauma and Orthopaedic Surgery, University Medical Center Hamburg-Eppendorf, Martinistraße 52, 20246 Hamburg, Germany (email: t.rolvien@uke.de and m.krause@uke.de, respectively).
*Department of Trauma and Orthopaedic Surgery, University Medical Center Hamburg-Eppendorf, Hamburg, Germany.
†Department of Osteology and Biomechanics, University Medical Center Hamburg-Eppendorf, Hamburg, Germany.
‡Department of Legal Medicine, University Medical Center Hamburg-Eppendorf, Hamburg, Germany.
J.S. and F.N.S. contributed equally to this article and therefore share first authorship.
Final revision submitted July 12, 2022; accepted July 27, 2022.
The authors declared that there are no conflicts of interest in the authorship and publication of this contribution. AOSSM checks author disclosures against the Open Payments Database (OPD). AOSSM has not conducted an independent investigation on the OPD and disclaims any liability or responsibility relating thereto.
Ethical approval for this study was obtained from the Ethik-Kommission der Ärztekammer-Hamburg (WF-165/20).

technique[1,19,28] were analyzed. For this purpose, each fibular scan was oriented with respect to the anteroposterior rotation around the long axis, and the center of mass was automatically calculated for each axial slice. Four neighboring columns were created out of the fibular stack. A combined analysis of the heights (VOIs) and columns allowed a determination of individual quadrants, with each quadrant being cropped respecting the Cartesian coordinate system with its origin aligned to the center of mass per slice. Finally, the bone microarchitecture parameters of the automatically segmented individual quadrants representing the entry and exit positions of the drill tunnels were compared: anatomic (anterolateral quadrant of VOI 2 to posteromedial quadrant of VOI 1) and nonanatomic (anterior quadrant of VOI 2 to posterior quadrant of VOI 2). Customized Python scripts were handled with the workflow manager XamFlow (Version 1.7.5.0; Lucid Concepts AG).

Statistical Analysis

Statistical analysis was performed using Prism (Version 8.4.0; GraphPad Software, Inc). Data were analyzed by ROUT test and significant outliers ($Q = 0.1\%$) excluded from further analysis. Normality distribution of the data was tested using the Shapiro-Wilk test, and for comparison between 2 groups, the Student t test or Mann-Whitney U test was used for parametric or nonparametric data, respectively. For the analysis of an association between age and bone microarchitectural parameters, linear regression analysis was performed, and the coefficient of determination (R^2) was calculated, as well as the regression slopes with confidence intervals. For comparisons of $\geq$3 groups, 1-way analysis of variance was carried out, including repeated measures with Tukey correction for parametric data or the Kruskal-Wallis test with the Dunn multiple-comparison test for nonparametric data. Repeated measures analysis of variance was used for paired analysis of bone microarchitecture parameters. Results are given as absolute values or mean and standard deviation. The level of significance was defined as $P < .05$. Exact P values are reported unless $P < .0001$.

RESULTS

Weight, height, and BMI did not differ significantly between women and men (Table 1). Most densitometric and microarchitectural parameters were not different between women and men. Only trabecular thickness was significantly lower in women than men (0.216 ± 0.015 vs 0.236 ± 0.020 mm; $P = .004$). Geometric indices were also significantly lower in women than men.

Evaluation of the age-related associations (Figure 1A) revealed a moderate to strong linear decline in volumetric BMD for the trabecular and cortical compartments in women (Tb.BMD, $R^2 = 0.698$, $P = .0002$; Ct.BMD, $R^2 = 0.361$, $P = .023$) (Figure 1B). In contrast, no association with age was observed in men for either densitometric or microarchitectural parameters except for Ct.BMD ($R^2 = 0.300$; $P = .034$) (Figure 1C). Regarding BMI-related changes, there were some positive associations in men, including Ct.BMD and Tb.N, whereas no associations between BMI and proximal fibular microarchitecture could be detected in women (Supplemental Figure S1, available online).

TABLE 1
Demographic and Bone Microarchitecture Parameters of the Proximal Fibula by Sex[a]

	Women (n = 15)	Men (n = 15)	P Value
Demographics			
Age, y	51.7 ± 20.0	51.5 ± 18.5	.985
Weight, kg	78.3 ± 19.6	78.9 ± 16.5	.931
Height, cm	170.8 ± 5.9	175.9 ± 9.4	.085
BMI	26.8 ± 6.7	25.5 ± 5.0	.530
Bone microarchitecture			
Tt.BMD, mg HA/cm^3	165.0 ± 62.7	162.5 ± 38.7	.897
Tb.BMD, mg HA/cm^3	106.6 ± 40.0	118.5 ± 34.2	.389
Ct.BMD, mg HA/cm^3	636.7 ± 112.1	658.1 ± 58.9	.522
BV/TV	0.155 ± 0.048	0.183 ± 0.054	.146
Tb.N, mm^{-1}	0.981 ± 0.244	0.943 ± 0.217	.651
Tb.Th, mm	0.216 ± 0.015	0.236 ± 0.020	**.004**
Ct.Th, mm	0.479 ± 0.140	0.497 ± 0.079	.679
Ct.Po	0.009 ± 0.007	0.008 ± 0.003	.769
Tt.Ar, mm^2	256.1 ± 73.9	353.7 ± 55.7	**.0003**
Tb.Ar, mm^2	233.2 ± 72.3	312.9 ± 62.6	**.004**
Ct.Ar, mm^2	24.6 ± 8.2	30.2 ± 5.4	**.041**
Ct.Pm, mm	65.4 ± 8.2	80.2 ± 6.7	**.003**

[a]Data are presented as mean ± SD. Bold P values indicate statistically significant difference between women and men ($P < .05$). BMI, body mass index; BV/TV, bone volume to tissue volume; Ct.Ar, cortical area; Ct.BMD, cortical bone mineral density; Ct.Pm, cortical perimeter; Ct.Po, cortical porosity; Ct.Th, cortical thickness; Tb.Ar, trabecular area; Tb.BMD, trabecular bone mineral density; Tb.N, trabecular number; Tb.Th, trabecular thickness; Tt.Ar, total area; Tt.BMD, total bone mineral density.

Analysis of microarchitectural differences in relation to height (ie, 4 VOIs from proximal to distal) (Figure 2, A and B) showed decreasing trabecular mineralization (Tb.BMD) and microarchitecture (BV/TV), while cortical parameters increased (Ct.BMD) or remained stable (Ct.Th, cortical porosity) from proximal to distal (Figure 2, C and D). Geometric parameters showed distinct differences of the trabecular and cortical area at the different heights (Figure 2E), with the smallest area located at the fibular tip. These findings could be replicated in both sexes (Supplemental Tables S1 and S2 and Figure S2, available online). Assessment of specific age-related patterns within the different heights revealed a decline of trabecular parameters within all heights, whereas cortical values declined predominantly at the most distal VOI 4 in women (Supplemental Figure S3A). In men, no significant associations with age were observed except for Ct.BMD in VOI 4 (Supplemental Figure S3B).

Evaluation of the bone microarchitecture according to axial quadrants corresponding to the regions used for drill tunnel positions during PLC reconstruction (Figure 3, A and B) showed superior values for densitometric and microarchitectural parameters in the anatomic fibular drill tunnel when comparing entry or exit drill regions with the Larson

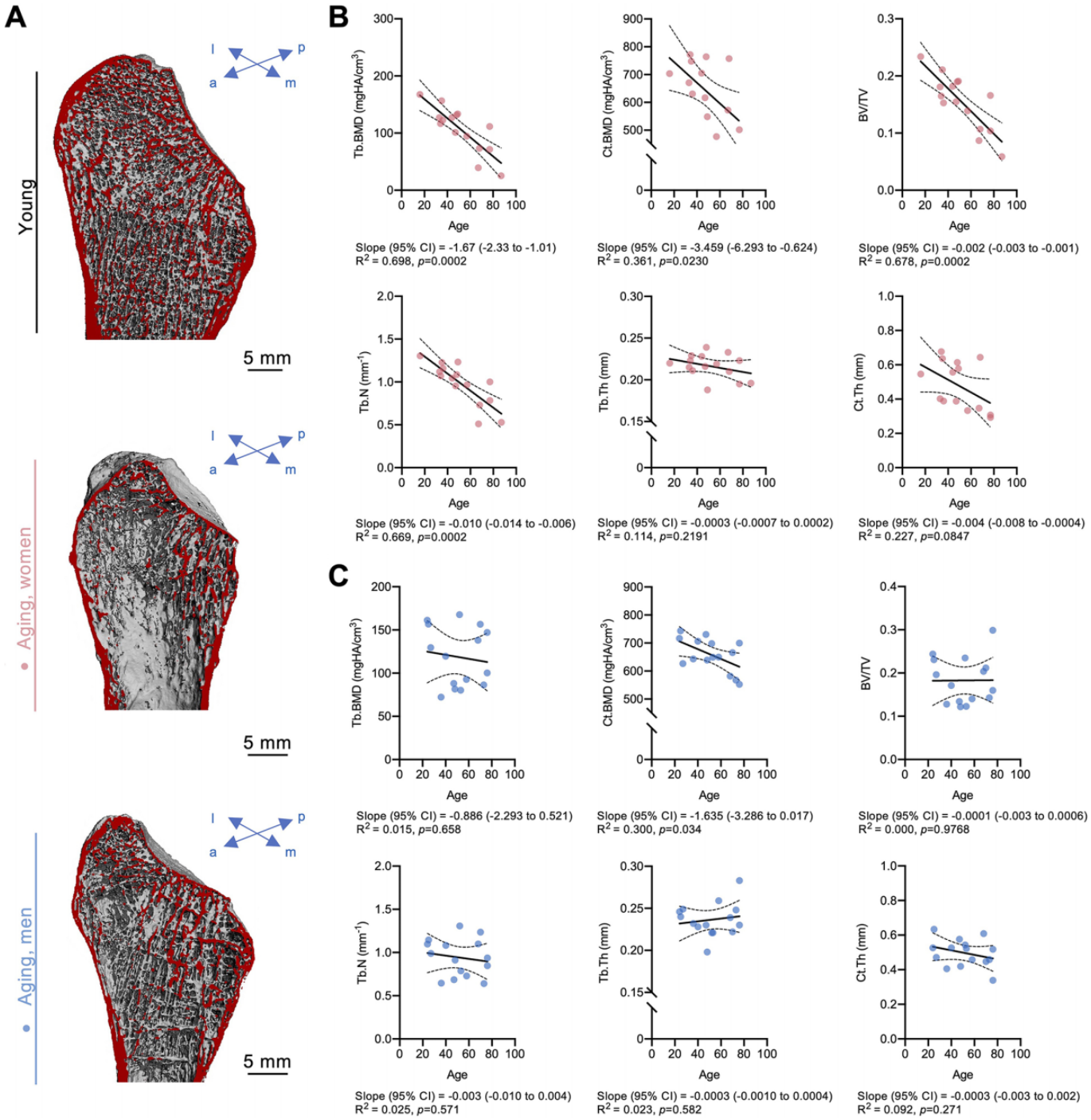

Figure 1. Age-related changes in trabecular and cortical bone microarchitecture in women vs men. (A) Representative 3-dimensional reconstructions of the proximal fibula in a young individual (top panel) and in a woman (middle panel) and a man (bottom panel) during aging. The virtual cut section is indicated in red. Associations between age and microarchitectural parameters in (B) women and (C) men. a, anterior; BV/TV, bone volume to tissue volume; Ct.BMD, cortical bone mineral density; Ct.Th, cortical thickness; l, lateral; m, medial; p, posterior; Tb.BMD, trabecular bone mineral density; Tb.N, trabecular number; Tb.Th, trabecular thickness.

technique (eg, BV/TV_{entry}, $P < .0001$; $Tb.N_{exit}$, $P < .0001$; $Ct.Th_{entry}$, $P < .0001$) (Figure 3C). For the exit point of the Larson technique, significant negative associations with age were revealed for BV/TV and Tb.N, whereas no associations were observed for the exit point of the anatomic procedures (Supplemental Figure S4, available online).

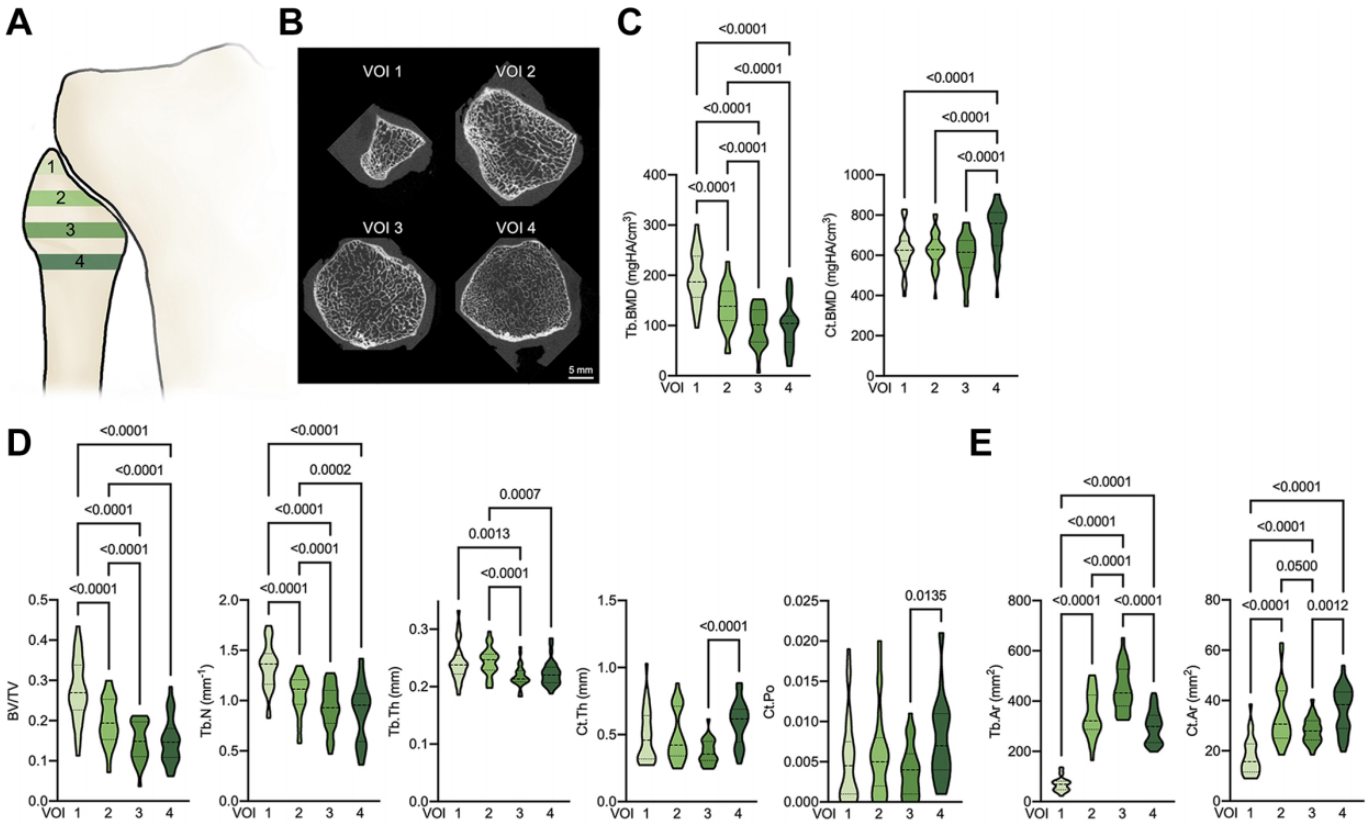

Figure 2. Fibular head microarchitecture parameters among different heights. (A) Schematic drawing (anterolateral view) with the 4 volumes of interest (VOIs 1-4) defined from proximal to distal and relative to the distance between the fibular tip and the distal end of the growth plate. (B) Examples of high-resolution peripheral quantitative computed tomography slices from the VOIs with visible differences in cortical and trabecular microarchitecture. Quantification and comparison of (C) densitometric parameters, (D) microarchitectural parameters, and (E) geometric parameters. The dashed lines of the truncated violin plots represent the median and quartiles. BV/TV, bone volume to tissue volume; Ct.Ar, cortical area; Ct.BMD, cortical bone mineral density; Ct.Po, cortical porosity; Ct.Th, cortical thickness; Tb.Ar, trabecular area; Tb.BMD, trabecular bone mineral density; Tb.N, trabecular number; Tb.Th, trabecular thickness.

DISCUSSION

Although the complexity of the PLC of the knee and its surgical care have been highlighted by previous reports,[5,17,31] no microarchitectural data existed on the proximal fibular microarchitecture and specific anatomy-based recommendations for fibula-based drill tunnel orientations until now. Significant differences were observed between women and men for the underlying association with age. Namely, moderate to strong negative associations between age and trabecular parameters were observed in women, whereas these associations were absent in men. Our findings further revealed distinct alterations in microarchitecture with respect to axial VOIs and columns. Importantly, microarchitecture parameters, including trabecular bone volume and Ct.Th, showed superior values in the fibular drill tunnel regions corresponding to the anatomic reconstruction techniques versus in the nonanatomic technique.

While an age-related decrease in bone microarchitecture is considered to occur in the skeleton in general, site-specific characteristics of the bone microarchitecture have been elaborated for different skeletal regions. In the clinical setting, the distal tibia and distal radius are routinely measured,[3,20,23,30,33] but also other skeletal sites or bones, such as the proximal tibia[13] or calcaneus,[22] have been investigated by HR-pQCT in the past. Only recently, the bone microarchitecture of the distal fibula has been studied by HR-pQCT by our group, demonstrating an age-related loss of bone microarchitecture in women but not men, which likely explains the higher susceptibility to distal fibular fractures in elderly women.[27,29] Consistent with these previous findings, women in this study showed a moderate to strong age-associated decrease in bone microarchitecture, which is in line with the high prevalence of osteoporosis in older women. However, the observed microarchitecture decline in the fibular head observed here was predominantly within the trabecular compartment, while the bone microarchitecture in the distal fibula showed cortical deterioration.[29] A reason for the compartment-specific decrease in microarchitecture could be the divergent mechanical environment in proximal versus distal regions.[7] Overall, it appears likely that impaired microarchitecture

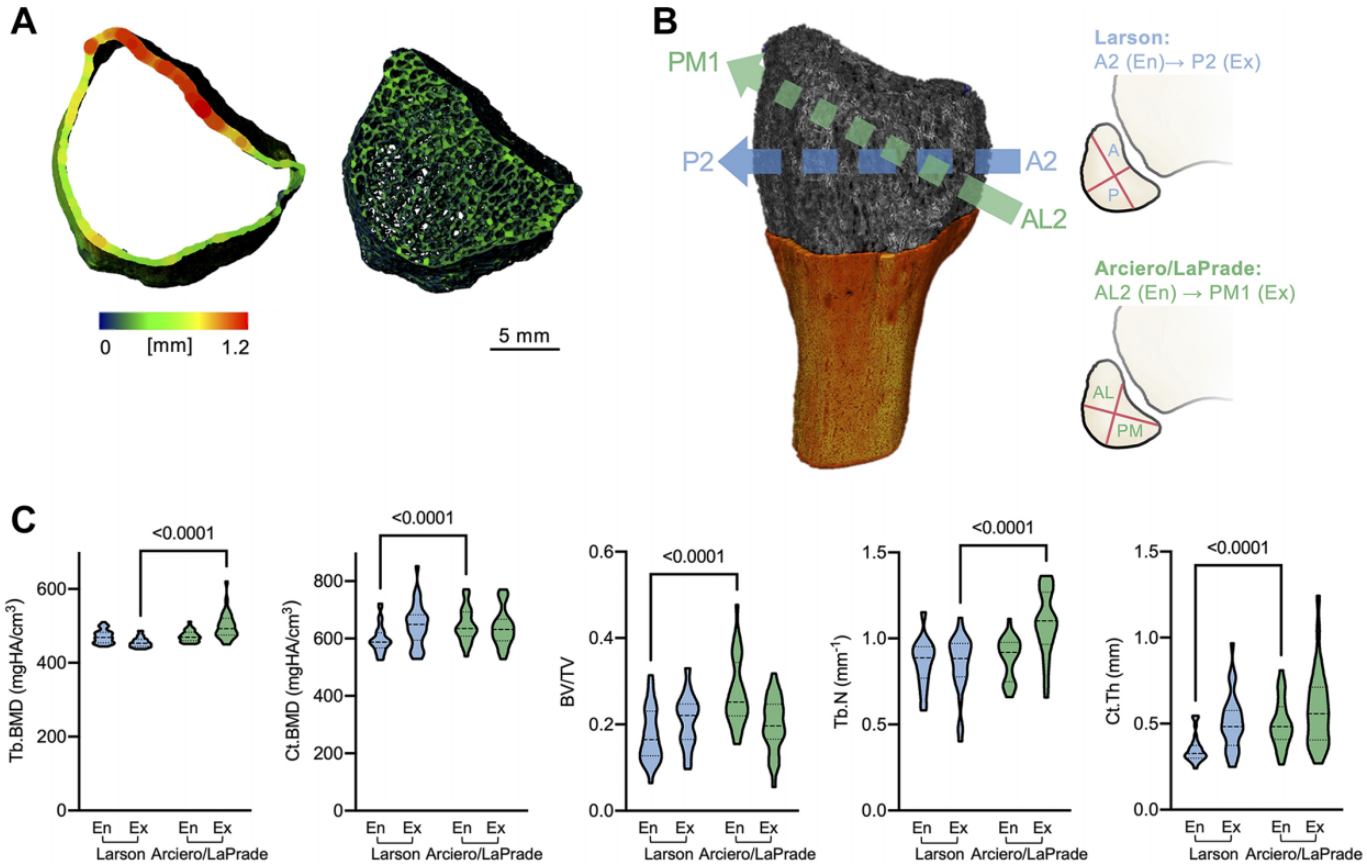

Figure 3. Variations in bone microarchitecture based on drill tunnel directions according to anatomic techniques vs Larson. (A) Representative axial view of segmentations of the cortical (left) and trabecular (right) bone compartments. The color coding indicates the thickness. (B) Demonstration of entry (En) and exit (Ex) points of the drill tunnels (left) in a 3-dimensional segmented scan and schematic axial slices. The letter and number (eg, A2) indicate the orientation and height (see Figure 2A). (C) Densitometric and microarchitectural parameters between En and Ex in the regions according to drill tunnels corresponding to anatomic techniques vs Larson. The dashed lines of the truncated violin plots represent the median and quartiles. A, anterior; AL, anterolateral; BV/TV, bone volume to tissue volume; Ct.BMD, cortical bone mineral density; Ct.Th, cortical thickness; P, posterior; PM, posteromedial; Tb.BMD, trabecular bone mineral density; Tb.N, trabecular number.

of the proximal fibula, as observed in older women, could increase susceptibility to, for example, arcuate fractures[12] and especially contribute to failure in surgical reconstruction of the PLC.

Specific subregions were analyzed to characterize the site-specific microarchitecture within the proximal fibula. The proximal fibular tip showed significantly lower bone area but overall preserved microarchitecture, illustrating that the skeletal quality in this region is likely not the leading reason for the skeletal-related failure of PLC reconstruction, such as graft cutout. Based on microarchitecture outcomes and regardless of the surgical technique, the ideal drill tunnel positions would most likely be in VOI 1 and VOI 2, given the favorable combination of preserved trabecular and cortical microarchitecture. Notably, cortical thickness was relevantly higher only in the region inferior to VOI 4 (ie, the diaphyseal region). Simulation of specific drill tunnel positions frequently used in PLC reconstruction was performed afterward. For the Larson technique,[19] a horizontal anteroposterior tunnel was simulated, contrasting the LaPrade or Arciero technique with an ascending tunnel from anterolateral to posteromedial.[1,28] While initial visualization suggested topographic differences in cortical and trabecular microarchitecture, customized segmentation with regional analysis revealed superior results for entry and exit quadrants for several microarchitecture parameters in the anatomic techniques (LaPrade/Arciero) as compared with the nonanatomic Larson technique. A reason for this difference could be that ligamentous attachments led to locally higher loading forces and thus represented a bone-anabolic stimulus. As the microarchitecture parameters corresponding to the Larson technique especially declined with age, older individuals might be at additional risk for failure with this technique. Given the growing functional demands of older individuals, these results appear clinically important.

Although anatomic PLC reconstruction techniques involving fibular drill tunnels as described by LaPrade or Arciero[21] may provide higher rotational stabilization than a nonanatomic technique, as in the Larson technique,[8]

anatomic reconstructions may also fail. A systematic review indicated a mean failure rate of 9.4% in PLC reconstruction or repair cases and 3 intraoperative fractures,[21] although the individual causes for failure were not often reported. Graft slippage and tunnel widening are acknowledged problems of transplant fixation in the proximal tibia in anterior cruciate ligament reconstruction, which has been attributed to decreased BMD,[2,16] large tunnel diameter,[4,26] and bone impaction.[15] From the collective results of previous studies and the present investigation, the clinical implication is that, although bone-related failure may occur, fibular drill tunnels have favorable microarchitectural support in anatomic reconstruction, possibly resulting in the observed low bone-related complication rates in young individuals. In this context, it should be noted that fibular fixation strength is only 1 reason for failure and that the biomechanical function of the grafts is highly dependent on their location.

Limitations

Our study has a few limitations. While HR-pQCT is a state-of-the-art technique with the best possible resolution in the context of a clinical microarchitecture analysis, no biomechanical tests could be performed in the current study setup. Additional biomechanical studies should evaluate cutout and/or tunnel widening in different drill tunnel positions, for example, by applying a defined cyclic tensile load. The individual contribution of the trabecular and cortical compartments within the fibular drill tunnels regarding stability as well as skeletal-related complications is not known. While we hypothesize that cortical thickness may be the major contributor to stability, this merits further investigation, including finite element modeling and biomechanical testing. Moreover, reproducibility in terms of intra- or interrater reliability was not assessed in this study. Nonetheless, excellent reproducibility of second-generation HR-pQCT regarding geometry, BMD, trabecular bone, and cortical thickness has been reported in a previous study.[6] Another limitation is that other surgical techniques or alternative drill tunnel positions for PLC reconstruction were not investigated. Although anatomic reconstructions (ie, LaPrade or Arciero) were associated with superior microarchitecture, this technique might not be applicable in all patients owing to intraoperative factors.

CONCLUSION

This study revealed that age represents a relevant risk factor for impaired skeletal microarchitecture in the proximal fibula in women but not men. Since the skeletal subregions around drill tunnels for PLC reconstruction according to LaPrade or Arciero showed superior bone microarchitecture as compared with those per Larson, it should now be explored whether this implies improved stability and lower failure rates attributed to skeletal complications such as fractures, graft cutout, or tunnel widening.

Supplemental material for this article is available at http://journals.sagepub.com/doi/suppl/10.1177/23259671221126475.

REFERENCES

1. Arciero RA. Anatomic posterolateral corner knee reconstruction. *Arthroscopy*. 2005;21(9):1147.
2. Brand JC Jr, Pienkowski D, Steenlage E, Hamilton D, Johnson DL, Caborn DN. Interference screw fixation strength of a quadrupled hamstring tendon graft is directly related to bone mineral density and insertion torque. *Am J Sports Med*. 2000;28(5):705-710.
3. Burt LA, Liang Z, Sajobi TT, Hanley DA, Boyd SK. Sex- and site-specific normative data curves for HR-pQCT. *J Bone Miner Res*. 2016;31(11):2041-2047.
4. Cain EL, Phillips BB, Charlebois SJ, Azar FM. Effect of tibial tunnel dilation on pullout strength of semitendinosus-gracilis graft in anterior cruciate ligament reconstruction. *Orthopedics*. 2005;28(8):779-783.
5. Chahla J, Murray IR, Robinson J, et al. Posterolateral corner of the knee: an expert consensus statement on diagnosis, classification, treatment, and rehabilitation. *Knee Surg Sports Traumatol Arthrosc*. 2019;27(8):2520-2529.
6. Chiba K, Okazaki N, Kurogi A, et al. Precision of second-generation high-resolution peripheral quantitative computed tomography: intra- and intertester reproducibilities and factors involved in the reproducibility of cortical porosity. *J Clin Densitom*. 2018;21(2):295-302.
7. Cointry GR, Nocciolino L, Ireland A, et al. Structural differences in cortical shell properties between upper and lower human fibula as described by pQCT serial scans: a biomechanical interpretation. *Bone*. 2016;90:185-194.
8. Domnick C, Frosch KH, Raschke MJ, et al. Kinematics of different components of the posterolateral corner of the knee in the lateral collateral ligament-intact state: a human cadaveric study. *Arthroscopy*. 2017;33(10):1821-1830, e1.
9. Feeley BT, Muller MS, Sherman S, Allen AA, Pearle AD. Comparison of posterolateral corner reconstructions using computer-assisted navigation. *Arthroscopy*. 2010;26(8):1088-1095.
10. Gelber PE, Drager J, Maheshwer B, et al. Large variability exists in the management of posterolateral corner injuries in the global surgical community. *Knee Surg Sports Traumatol Arthrosc*. 2020;28(7):2116-2123.
11. Grimm NL, Levy BJ, Jimenez AE, Bell R, Arciero RA. Open anatomic reconstruction of the posterolateral corner: the Arciero technique. *Arthrosc Tech*. 2020;9(9):e1409-e1414.
12. Huang GS, Yu JS, Munshi M, et al. Avulsion fracture of the head of the fibula (the "arcuate" sign): MR imaging findings predictive of injuries to the posterolateral ligaments and posterior cruciate ligament. *AJR Am J Roentgenol*. 2003;180(2):381-387.
13. Kadri A, Binkley N, Hare KJ, Anderson PA. Bone health optimization in orthopaedic surgery. *J Bone Joint Surg Am*. 2020;102(7):574-581.
14. Keen CE, Whittier DE, Firminger CR, Edwards WB, Boyd SK. Validation of bone density and microarchitecture measurements of the load-bearing femur in the human knee obtained using in vivo HR-pQCT protocol. *J Clin Densitom*. 2021;24(4):651-657.
15. Kold S, Bechtold JE, Ding M, Chareancholvanich K, Rahbek O, Soballe K. Compacted cancellous bone has a spring-back effect. *Acta Orthop Scand*. 2003;74(5):591-595.
16. Krause M, Hubert J, Deymann S, et al. Bone microarchitecture of the tibial plateau in skeletal health and osteoporosis. *Knee*. 2018;25(4):559-567.
17. LaPrade RF, Ly TV, Wentorf FA, Engebretsen L. The posterolateral attachments of the knee: a qualitative and quantitative morphologic analysis of the fibular collateral ligament, popliteus tendon, popliteofibular ligament, and lateral gastrocnemius tendon. *Am J Sports Med*. 2003;31(6):854-860.

18. LaPrade RF, Wentorf FA, Fritts H, Gundry C, Hightower CD. A prospective magnetic resonance imaging study of the incidence of posterolateral and multiple ligament injuries in acute knee injuries presenting with a hemarthrosis. *Arthroscopy*. 2007;23(12):1341-1347.
19. Larson RV. Isometry of the lateral collateral and popliteofibular ligaments and techniques for reconstruction using a free semitendinosus tendon graft. *Oper Tech Sports Med*. 2001;9(2):84-90.
20. Macdonald HM, Nishiyama KK, Hanley DA, Boyd SK. Changes in trabecular and cortical bone microarchitecture at peripheral sites associated with 18 months of teriparatide therapy in postmenopausal women with osteoporosis. *Osteoporos Int*. 2011;22(1):357-362.
21. Maheshwer B, Drager J, John NS, Williams BT, LaPrade RF, Chahla J. Incidence of intraoperative and postoperative complications after posterolateral corner reconstruction or repair: a systematic review of the current literature. *Am J Sports Med*. 2021;49(12):3443-3452.
22. Metcalf LM, Dall'Ara E, Paggiosi MA, et al. Validation of calcaneus trabecular microstructure measurements by HR-pQCT. *Bone*. 2018; 106:69-77.
23. Milovanovic P, Adamu U, Simon MJ, et al. Age- and sex-specific bone structure patterns portend bone fragility in radii and tibiae in relation to osteodensitometry: a high-resolution peripheral quantitative computed tomography study in 385 individuals. *J Gerontol A Biol Sci Med Sci*. 2015;70(10):1269-1275.
24. Noyes FR, Barber-Westin SD, Albright JC. An analysis of the causes of failure in 57 consecutive posterolateral operative procedures. *Am J Sports Med*. 2006;34(9):1419-1430.
25. Püschel K. Lehre und Forschung an Verstorbenen. *Rechtsmedizin*. 2016;26(2):115-119.
26. Sauer S, Lind M. Bone tunnel enlargement after ACL reconstruction with hamstring autograft is dependent on original bone tunnel diameter. *Surg J (N Y)*. 2017;3(2):e96-e100.
27. Schlickewei C, Schweizer C, Puschel K, et al. Age-, sex-, and subregion-specific properties of distal fibular microarchitecture and strength: an ex vivo HR-pQCT study. *J Orthop Res*. Published online May 3, 2022. doi:10.1002/jor.25351
28. Serra Cruz R, Mitchell JJ, Dean CS, Chahla J, Moatshe G, LaPrade RF. Anatomic posterolateral corner reconstruction. *Arthrosc Tech*. 2016;5(3):e563-e572.
29. Stürznickel J, Schmidt FN, Schafer HS, et al. Bone microarchitecture of the distal fibula assessed by HR-pQCT. *Bone*. 2021; 151:116057.
30. Warden SJ, Liu Z, Fuchs RK, van Rietbergen B, Moe SM. Reference data and calculators for second-generation HR-pQCT measures of the radius and tibia at anatomically standardized regions in White adults. *Osteoporos Int*. 2022;33(4):791-806.
31. Weiss S, Krause M, Frosch KH. Posterolateral corner of the knee: a systematic literature review of current concepts of arthroscopic reconstruction. *Arch Orthop Trauma Surg*. 2020;140(12):2003-2012.
32. Whittier DE, Boyd SK, Burghardt AJ, et al. Guidelines for the assessment of bone density and microarchitecture in vivo using high-resolution peripheral quantitative computed tomography. *Osteoporos Int*. 2020;31(9):1607-1627.
33. Whittier DE, Burt LA, Hanley DA, Boyd SK. Sex- and site-specific reference data for bone microarchitecture in adults measured using second-generation HR-pQCT. *J Bone Miner Res*. 2020;35(11): 2151-2158.